

H.L. SENG<sup>1,✉</sup>  
T. OSIPOWICZ<sup>1</sup>  
J. ZHANG<sup>2</sup>  
E.S. TOK<sup>3</sup>

# Observation of local lattice tilts in strain-relaxed Si<sub>1-x</sub>Ge<sub>x</sub> using high resolution channeling contrast microscopy

<sup>1</sup> Department of Physics, Centre for Ion Beam Applications, National University of Singapore, 2 Science Drive 3, Singapore 117542, Singapore  
<sup>2</sup> Department of Physics, Centre for Electronic Materials and Devices, Imperial College of Science, Technology and Medicine, Blackett Laboratory, Prince Consort Road, London SW7 2BW, UK  
<sup>3</sup> Department of Material Science, National University of Singapore, 10 Science Drive 4, Lower Kent Ridge Road, Singapore 117543, Singapore

Received: 16 June 2004/Accepted: 29 September 2004  
Published online: 18 November 2004 • © Springer-Verlag 2004

**ABSTRACT** A ‘cross-hatch’ morphology is often seen in strain-relaxed Si<sub>1-x</sub>Ge<sub>x</sub> virtual substrates grown using the compositional grading technique. High resolution channeling contrast microscopy measurements, which probe both laterally and vertically into the structure, have revealed the association of such cross-hatch patterns with local lattice-plane bending. In this work, we report the influence of the growth temperature on the extent of the local lattice tilts determined from the channeling contrast measurements. Lines of pileup threading dislocations observed on the surface have also been imaged for the first time, providing us with information on their influence on the lattice-tilt arrangements and orientations.

PACS 82.80.Yc; 61.85.+p; 68.55.Jk

## 1 Introduction

Strained layers offer the ability to modify the energy band gap and to tailor the transport and optical properties of a semiconductor. In particular, a strained SiGe layer, when used in a heterojunction field-effect transistor, enhances the hole mobility [1, 2]. Devices with a strained Si channel grown on a relaxed SiGe buffer layer are promising candidates for the realization of both electron- and hole-mobility enhancement [2–7]. Integrated optoelectronics is another promising research field for SiGe/Si heterodevices. Relaxed SiGe buffers are used as templates for integrating III–V materials with Si, thus expanding the potential of Si optoelectronics [4, 8–10].

In growing a high quality strain relaxed SiGe layer, two important criteria are a low threading dislocation density and a smooth surface. There are a number of ways to achieve this [11, 12], and one of the more successful approaches that results in a fully strain-relaxed layer with low threading dislocation density is by incorporating an intermediate compositionally graded buffer layer [4, 13–16]. This involves growing a linearly graded buffer up to the desired Ge concentration prior to the growth of a relaxed constant-composition

SiGe layer. Unfortunately, a cross-hatch pattern that is oriented along the orthogonal [110] directions often results from the growth. Such cross-hatch roughening affects carrier mobility and the quality of the layers subsequently grown on the strain-relaxed buffer layer. A good understanding of the strain-relaxation effects and the influence of different growth conditions on the surface morphology is important for device fabrication.

The cross-hatch morphology has been studied using high resolution channeling contrast microscopy (CCM) [17], which probes both laterally and vertically into the structure. In previous work [18] on similar samples, reversal of the channeling contrast with tilting of the sample with respect to the ion-beam direction has revealed the association of the cross-hatch features with lattice-plane bending. In this work, we report the influence of the growth temperature on the extent of the local lattice tilts. Lines of pileup threading dislocations observed on the surface have also been imaged for the first time, providing us with information on their influence on the lattice-tilt arrangements and orientations.

## 2 Experimental

The samples investigated were grown using a modified gas source molecular beam epitaxy (GSMBE) system [19]. The nominal sample structure consists of a linearly graded (LG) Si<sub>1-x</sub>Ge<sub>x</sub> layer, from  $x = 5\%$  to a final Ge composition of 22% (with a grading rate increasing by 7% Ge per  $\mu\text{m}$ ) followed by a 1.2- $\mu\text{m}$ -thick constant-composition (CC) Si<sub>0.8</sub>Ge<sub>0.2</sub> layer and a 5-nm-thick Si cap layer. The LG and CC layer-growth temperatures were varied as given in Table 1.

|   | Sample A          | Sample B          | Sample C            |
|---|-------------------|-------------------|---------------------|
| LG growth temperature (°C)                        | 800               | 800               | 600                 |
| CC growth temperature (°C)                        | 800               | 600               | 600                 |
| Minimum yield (%)                                 | 4.5               | 3.6               | 5.9                 |
| Range of lattice tilts (°)                        | 0.15              | 0.14              | 0.26                |
| Threading dislocation density (cm <sup>-2</sup> ) | $7.6 \times 10^4$ | $6.5 \times 10^4$ | $> 3.0 \times 10^5$ |

TABLE 1 Growth conditions and measured values

✉ Fax: +65-67776126, E-mail: physengd@nus.edu.sg

The overall crystalline qualities of the layers were determined from broad beam channeling measurements using a 2-MeV  $\text{He}^+$  beam with spot size of  $\sim 1 \text{ mm}^2$  and beam current of  $\sim 10 \text{ nA}$ . Rutherford backscattering (RBS) spectra in channeled and nonchanneled alignment were recorded with a 50-mm<sup>2</sup> passivated implanted planar silicon (PIPS) detector of 14-keV energy resolution at 160° scattering angle. The axial minimum channeling yield,  $\chi_{\text{min}}$ , was taken from the ratio of the channeled to the random spectra corresponding to a depth of 100 nm. For CCM measurements, a focused ion beam of  $\sim 1\text{-}\mu\text{m}^2$  spot size and beam current of  $\sim 100 \text{ pA}$  is scanned over a region of the sample. A 300-mm<sup>2</sup> PIPS detector of 19-keV energy resolution at 145° scattering angle, which gives a larger solid angle of  $\sim 280 \text{ msr}$ , is used in order to accumulate reasonable statistics during the one-hour runs for each spectrum. RBS spectra with the beam at (001) axial alignment and at  $\pm 0.3^\circ$  off the (001) axis in the [110] direction in steps of  $0.1^\circ$  were recorded in list-mode format to allow off-line analysis. CCM maps were later generated from the RBS spectra at a corresponding depth interval of  $\sim 0.6 \mu\text{m}$  from the CC layer.

The local lattice-tilt angles across the scanned area are determined by examining several CCM maps collected at different sample-rotation angles. The procedures for extracting the local tilt angles are described here and illustrated in Fig. 1. Intensity as a function of lateral position is first extracted from all CCM maps collected at different sample-rotation angles  $\theta_i$  and from the same selected region of the sample surface. The intensity profile is obtained by projecting (summing) the

counts vertically from a selected region 'A' that excludes horizontal bands of contrast of the CCM image. This is indicated in Fig. 1a for a CCM map of sample C. Next, graphs of normalized yield (pixel counts) against sample-rotation angles are plotted for horizontal 5- $\mu\text{m}$  intervals in the scanned area. Figure 1b shows the line-intensity profiles extracted from region 'A' for  $\theta = +0.3^\circ, 0^\circ$  and  $-0.3^\circ$ . A Gaussian curve is then fitted to the data points for each graph. The local lattice-tilt angle,  $\phi$ , at every 5- $\mu\text{m}$  lateral position is obtained from the sample-rotation angle corresponding to the local minimum backscattered yield. Graphs of counts against sample-rotation angles for three positions are given in Fig. 1c. The range of lattice tilts is then determined from the difference between the maximum and minimum local tilt angles found.

### 3 Results and discussion

Differential interference contrast optical images reveal typical cross-hatch patterns along orthogonal [110] directions across the whole of the sample surfaces (Fig. 2a) for all samples. Lines of pileup dislocations (Fig. 2b) along orthogonal [110] directions are observed in sample C, which is grown at a low CC and LG layer growth temperature of 600 °C.

Figure 3 shows a CCM map at  $-0.2^\circ$  off the (001) axis for sample C, which excludes the lines of pileup threading dislocations. The lattice-tilt angles  $\phi$  extracted are plotted as a function of lateral distance across the sample to show the extent and orientation of the local lattice-plane tilts about the

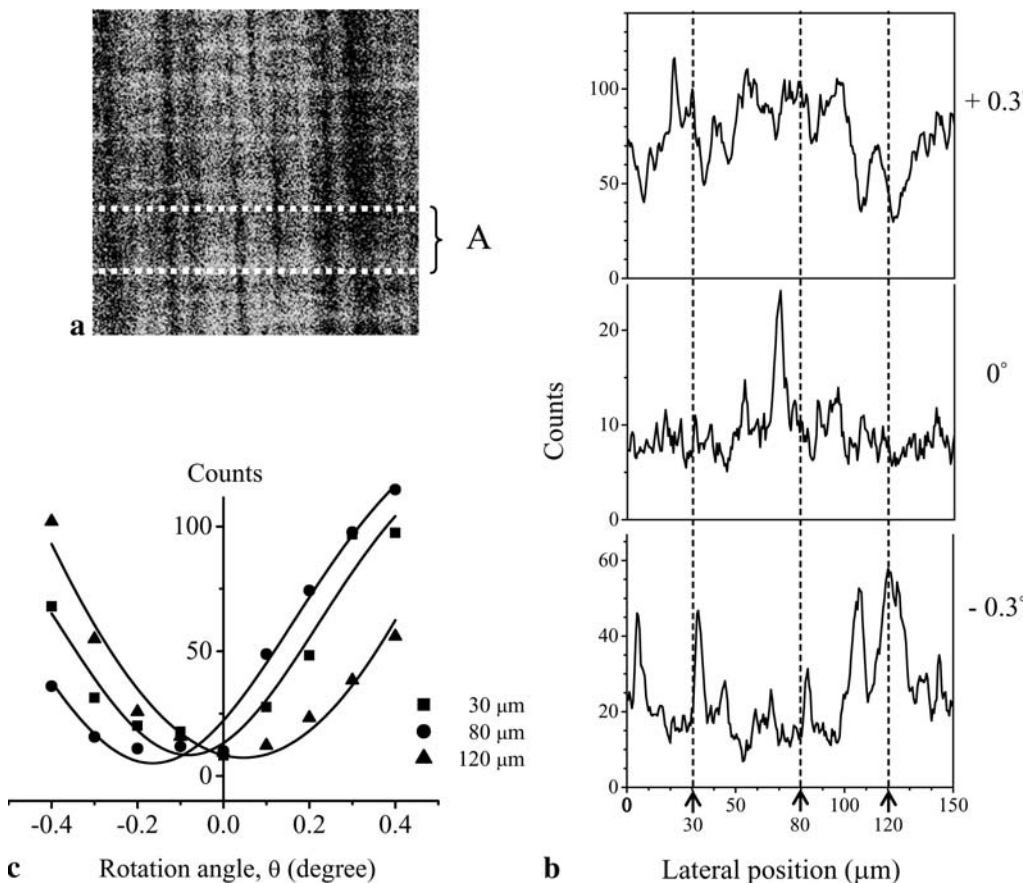
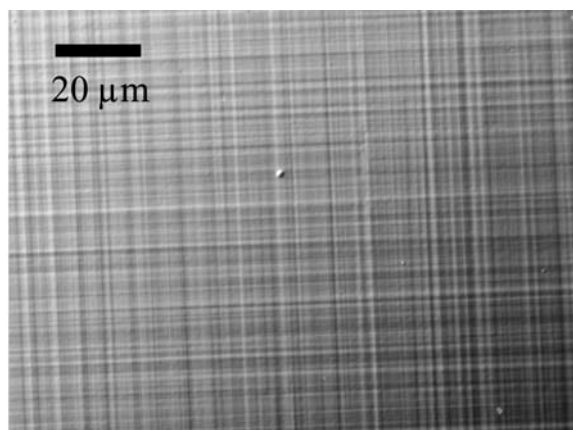
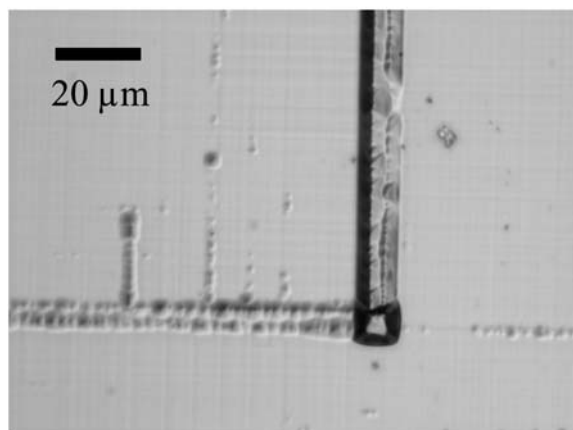


**FIGURE 1** a  $150 \times 150 \mu\text{m}^2$  CCM map of sample C at sample rotation of  $+0.3^\circ$ . Region 'A' indicates the area selected for extracting the line-intensity profiles. b Line-intensity profiles extracted from region A for  $\theta = +0.3^\circ, 0^\circ$  and  $-0.3^\circ$ . c Graphs of counts against sample-rotation angle for three positions indicated



a

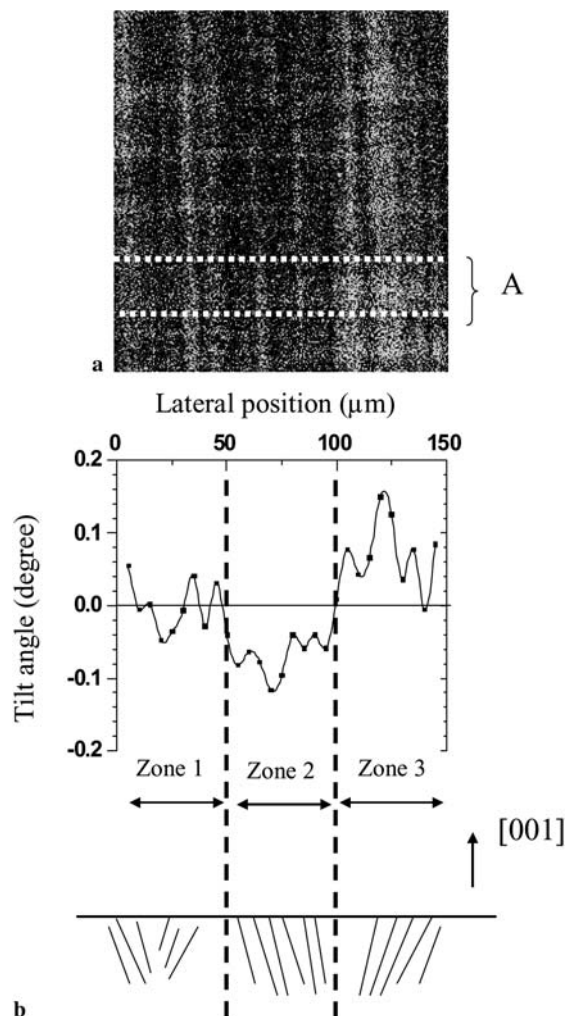


b

**FIGURE 2** a Differential interference contrast image of sample A showing typical cross-hatch morphology. b Differential interference contrast image of sample C showing lines of pileup threading dislocations

[110] directions across the scanned area. From the plot, we observe that there are three clearly different zones of average lattice tilts. In each zone, bright and dark bands in the CCM map are present, indicating that there is a variation in the lattice tilt along the  $[1\bar{1}0]$  direction. A schematic of the arrangement of the tilted planes within different zones is also shown in Fig. 3.

Table 1 gives the values of the range of tilts about the [110] directions for all samples. The range of tilts appears to be influenced by the growth temperature of the LG layer and is independent of the CC layer-growth temperature. At a lower LG layer-growth temperature of 600 °C a significantly larger lattice-tilt range is obtained compared to the other two samples. This is consistent with the idea that dislocations are mainly generated and confined in the graded layer [14, 20] and the range of the lattice tilts is therefore possibly affected by the interactions of the dislocations in this layer. Dislocation gliding, which is one of the strain-relaxation mechanisms, is not as efficient at a low temperature. Additional misfit dislocations may therefore have to be nucleated to relieve the misfit strain. The threading dislocation densities were estimated using the Schimmel etch method [21] and values for all samples are tabulated in Table 1. A higher threading dislocation density was obtained for sample C compared to the other two samples. The implication is that, at a lower growth temperature, the dislo-



b

**FIGURE 3** 150 × 150 μm<sup>2</sup> CCM map at sample rotation of -0.2° and graph of lattice tilt about [110] directions against lateral position for sample C

cation glide velocity is reduced, increasing the nucleation of misfit dislocations and hence increasing the density of threading arms in the layer. With a greater number of threading arms interacting at lower growth temperatures, there is a greater probability for the threading arms to be pinned and for dislocation pileup to result. Significant dislocation pileups have in fact been observed at the sample surface in the optical micrographs for this sample (Fig. 2b). From broad-beam RBS channeling measurements, it was found that the minimum yield,  $\chi_{\min}$ , is inversely correlated to the LG layer-growth temperature, indicating that a highly ordered layer with a small range of tilt is achieved at higher growth temperatures.

Because the CCM technique allows one to study selective regions of the sample using a focused beam, it enables lateral resolution of structures of the type seen in Fig. 2b to be analyzed. CCM measurements were therefore carried out in a region centered at the intersection of two lines of dislocation pileups. Figure 4 shows the CCM images at  $\langle 001 \rangle$  axial and rotated  $\pm 0.3^\circ$  off-axis about the orthogonal [110] directions. The two lines of pileup threading dislocations (labeled 'A' and 'B') show up as bright bands in the CCM map at axial alignment, indicating higher ion dechanneling near the dis-

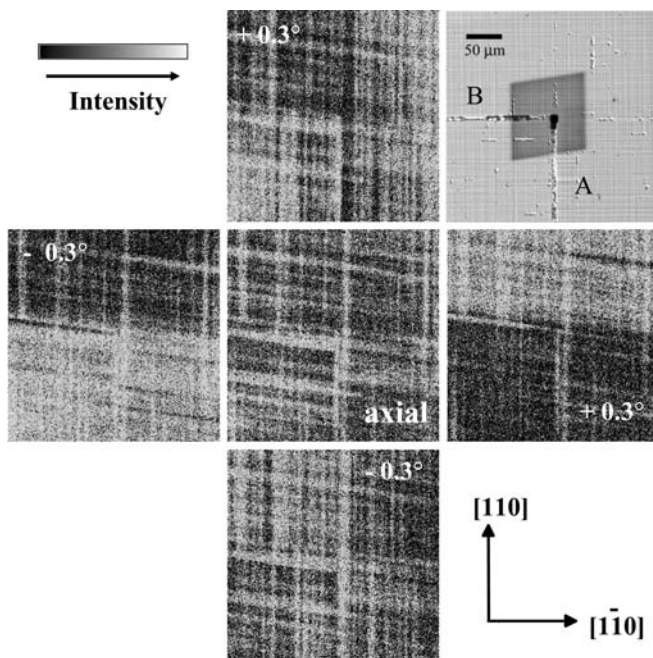


**FIGURE 4**  $300 \times 300 \mu\text{m}^2$  CCM images, at axial (*center*) and rotated  $\pm 0.3^\circ$  off axial about  $[1\bar{1}0]$  (*left/right*) and  $[110]$  (*top/bottom*) directions, centered at the intersection of two lines of dislocation pileups. An optical image of the same region is given in the *top right corner*

location pileups. In areas away from the dislocation pileups, a typical cross-hatch contrast is observed. On rotation of the sample off-axis in the horizontal and vertical directions, a reversal in the channeling contrast is observed. In addition, two distinct regions of opposite bright and dark contrast extending several hundreds of microns can be identified. The results suggest that the lines of dislocation pileups separate two large domains of opposing lattice tilts. These large domains of lattice tilts were found to extend through the constant-composition layer, as observed from CCM maps extracted at different energy (depth) windows. Such a large area of tilted regions of the same orientations could be partly accountable for the higher range of lattice tilts obtained for this sample. The exact nature of the strain-relaxation mechanisms responsible for the emergence of long range ordered tilt regions is still under investigation.

#### 4 Conclusions

CCM has been used to image the cross-hatch features observed in SiGe virtual substrates and also specific

areas of interest containing the lines of pileup threading dislocations. The range of the lattice tilts associated with the cross-hatch features was also determined from the CCM measurements. They were found to be influenced by the LG layer growth temperature. Lower temperature results in a larger range of tilts, a higher threading dislocation density and dislocation pileup. This suggests that for growth of high quality strain relaxed layers with low threading dislocation densities, a higher LG growth temperature is preferred. CCM measurements on regions with lines of pileup dislocations have suggested that these large lattice tilts produced at low LG temperature can be attributed to the large domains of lattice tilts extending several hundreds of microns, separated by the lines of dislocation pileups.

#### REFERENCES

- 1 U. Konig, H. Daembkes: *Solid-State Electron.* **38**, 1595 (1995)
- 2 F. Schäffler: *Semicond. Sci. Technol.* **12**, 1515 (1997)
- 3 R. People: *IEEE J. Quantum Electron.* **QE-22**, 1696 (1986)
- 4 E.A. Fitzgerald, Y.-H. Xie, D. Monroe, P.J. Silverman, J.M. Kuo, A.R. Kortan, F.A. Thiel, B.E. Weir: *J. Vac. Sci. Technol. B* **10**, 1807 (1992)
- 5 U. Konig, F. Schäffler: *Electron Device Lett.* **14**, 205 (1993)
- 6 D.K. Nayak, S.K. Chun: *Appl. Phys. Lett.* **64**, 2514 (1994)
- 7 C.K. Maiti, L.K. Bera, S. Chattopadhyay: *Semicond. Sci. Technol.* **13**, 1225 (1998)
- 8 R.M. Sieg, S.A. Ringel, S.M. Ting, S.B. Samavedan, M. Currie, T. Langdo, E.A. Fitzgerald: *J. Vac. Sci. Technol. B* **16**, 1471 (1998)
- 9 S.B. Samavedan, M.T. Currie, T.A. Langdo, E.A. Fitzgerald: *Appl. Phys. Lett.* **73**, 2125 (1998)
- 10 J.A. Carlin, M.K. Hudiat, S.A. Ringel, D.M. Wilt, E.B. Clark, C.W. Leitz, M. Currie, T. Langdo, E.A. Fitzgerald: in *Rec. Twenty-Eighth IEEE Photovoltaic Specialist Conf., 2000*, p. 1006
- 11 Y.H. Luo, J.L. Liu, G. Jin, K.L. Wang, C.D. Moore, M.A. Goorsky, C. Chih, K.N. Tu: *J. Electron. Mater.* **29**, 950 (2000)
- 12 A. Nishida, K. Nakagawa, E. Murakami, M. Miyao: *J. Appl. Phys.* **71**, 5913 (1992)
- 13 B.S. Meyerson, K.J. Uram, F.K. Le Goues: *Appl. Phys. Lett.* **53**, 2555 (1988)
- 14 F.K. LeGoues, B.S. Meyerson, J.F. Morar: *Phys. Rev. Lett.* **66**, 2903 (1991)
- 15 E.A. Fitzgerald, Y.H. Xie, M.L. Green, D. Brasen, A.R. Kortan, Y.J. Mii, J. Michel, B.W. Weir: *Appl. Phys. Lett.* **59**, 811 (1991)
- 16 P.M. Mooney, J.L. Jordan-Sweet, K. Ismail, J.O. Chu, R.M. Feenstra, F.K. Le Goues: *Appl. Phys. Lett.* **67**, 2373 (1995)
- 17 M.B.H. Breese, D.N. Jamieson, P.J.C. King: *Materials Analysis Using a Nuclear Microprobe* (Wiley, New York 1996)
- 18 H.L. Seng, T. Osipowicz, T.C. Sum, E.S. Tok, G. Breton, N.J. Woods, J. Zhang: *Appl. Phys. Lett.* **80**, 2940 (2002)
- 19 N.J. Woods, G. Breton, H. Graoui, J. Zhang: *J. Cryst. Growth* **227–228**, 735 (2001)
- 20 F.K. Le Goues, B.S. Meyerson, J.F. Morar, P.D. Kirchner: *J. Appl. Phys.* **71**, 4230 (1992)
- 21 D. Schimmel: *J. Electrochem. Soc.* **126**, 479 (1979)